Influence of ^{60}Co gamma radiation on fluorine plasma treated enhancement-mode high-electron-mobility transistor*

Quan Si(全 思)†, Hao Yue(郝 跃), Ma Xiao-Hua(马晓华), and Yu Hui-You(于惠游)

Key Laboratory of Wide Band Gap Semiconductor Materials and Devices, Institute of Microelectronics, Xidian University, Xi'an 710071, *China*

(Received 9 November 2010; revised manuscript received 6 December 2010)

AlGaN/GaN depletion-mode high-electron-mobility transistor (D-HEMT) and fluorine (F) plasma treated enhancement-mode high-electron-mobility transistor (E-HEMT) are exposed to ^{60}Co gamma radiation with a dose of 1.6 Mrad (Si). No degradation is observed in the performance of D-HEMT. However, the maximum transconductance of E-HEMT is increased after radiation. The 2DEG density and the mobility are calculated from the results of capacitance–voltage measurement. The electron mobility decreases after fluorine plasma treatment and recovers after radiation. Conductance measurements in a frequency range from 10 kHz to 1 MHz are used to characterize the trapping effects in the devices. A new type of trap is observed in the F plasma treated E-HEMT compared with the D-HEMT, but the density of the trap decreases by radiation. Fitting of $G_{\rm p}/\omega$ data yields the trap densities $D_{\rm T} = (1-3) \times 10^{12}$ cm$^{-2}\cdot$ eV^{-1} and $D_{\rm T} = (0.2-0.8) \times 10^{12}$ cm$^{-2}\cdot$eV^{-1} before and after radiation, respectively. The time constant is 0.5 ms–6 ms. With F plasma treatment, the trap is introduced by etch damage and degrades the electronic mobility. After ^{60}Co gamma radiation, the etch damage decreases and the electron mobility is improved. The gamma radiation can recover the etch damage caused by F plasma treatment.

Keywords: AlGaN/GaN, enhancement-mode high-electron-mobility transistors, fluorine plasma treatment, ^{60}Co gamma radiation

PACS: 85.30.De, 85.50.–n **DOI:** 10.1088/1674-1056/20/5/058501

1. Introduction

Enhancement-mode III-nitride high-electron-mobility transistor (HEMT), with a positive threshold voltage, is a key component for high-speed power switch, high temperature GaN integrated circuit [1] and high radiation resisted integrated circuit. Fluorine (F) plasma treatment[2] is a robust approach to controlling the threshold voltage of AlGaN/GaN HETM.[3−5] This technique has been demonstrated to shift the threshold voltage of AlGaN/GaN HEMTs toward a positive bias, thus enabling enhancement-mode operation.[6−9] It was reported that the fluorine plasma treatment enhancement-mode HEMT has a high stability under electronic stress and high temperature stress.[10,11] The radiation reliability[12,13] of fluorine plasma treatment enhancement-mode HEMT has not been studied.

In this paper, conventional depletion-mode HEMTs and fluorine plasma treatment enhancement-mode HEMTs are exposed to ^{60}Co gamma radiation with a dose of 1.6 Mrad (Si). The results of D-HEMTs show no degradation, however, the maximum drain current and the maximum transconductance of E-HEMTs increase after radiation. Capacitance and conductance measurements are used to study the mechanism. The ^{60}Co gamma radiation reduces the trap in E-mode HEMT generated by fluorine plasma treatment and recovers the maximum transconductance of E-HEMT.

2. Device and fabrication

The AlGaN/GaN HEMT layer was grown by metal organic chemical vapour deposition (MOCVD) on a sapphire substrate. The heterostructure was composed of a nucleation layer, a 1 μm-thick GaN buffer layer and an un-doped 20-nm-thick AlGaN barrier layer. An AlN mole fraction of AlGaN was 30%. Step-and-repeat system was used to open the gate regions of AlGaN/GaN D-HEMTs and Al-

*Project supported by the National Natural Science Foundation of China (Grant No. 60736033) and the Fundamental Research Funds for the Central Universities, China (Grant No. JY10000904009).

†Corresponding author. E-mail: siquan@163.com

© 2011 Chinese Physical Society and IOP Publishing Ltd

GaN/GaN E-HEMTs separately on one wafer. These processes have been described in detail in our previous paper.[11] The device fabrication started with mesa isolation which had been formed by inductively coupled plasma (ICP) with an etch-depth of 200 nm. Ohmic contacts consisting of Ti/Al/Ni/Au (22 nm/140 nm/55 nm/45 nm) were annealed in a nitrogen ambient at 850°, yielding a contact resistance typically around 1.0 Ω·mm. The Schottky contacts were formed by Ni/Au. Before the gate deposition of the AlGaN/GaN E-HEMTs, the wafer was treated by CF_4 plasma (150 W, 150 s) in a reactive ion etching (RIE) system. Direct current characteristics were investigated by Agilent 1500B semiconductor parameter analyzer, capacitance–voltage and capacitance–frequency were measured by Keythley 4200.

3. Radiation and measurement

The threshold voltages are typically 0.57 V and −3.5 V for the AlGaN/GaN E-HEMTs and AlGaN/GaN D-HEMTs, respectively. The transconductance peak values of AlGaN/GaN E-HEMTs and AlGaN/GaN D-HEMTs are 201 mS/mm and 234 mS/mm, respectively (Figs. 1 and 2) . The DC characteristics obtained are consistent with those reported before.[6,7,14]

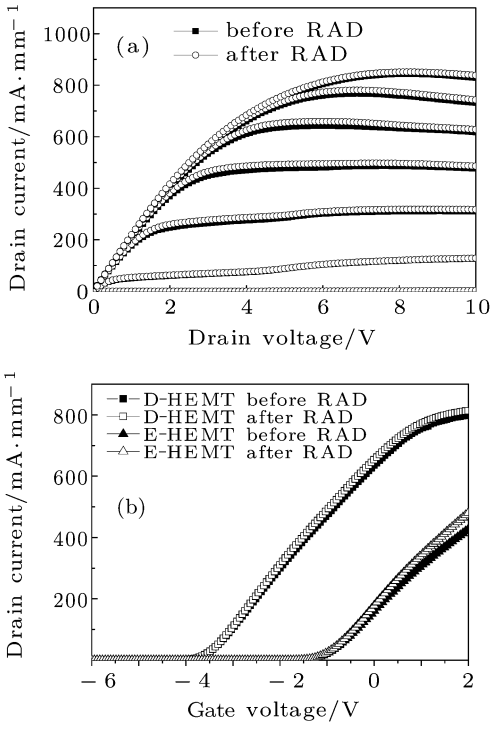


Fig. 1. (a) DC I–V output characteristics and (b) transfer characteristics of AlGaN/GaN D-HEMT and E-HEMT before and after ^{60}Co gamma radiation.

D-HEMTs and E-HEMTs are all exposed to ^{60}Co gamma radiation with a dose of 1.6 Mrad (Si), the results (Figs. 1 and 2) show no degradation in D-HEMT after radiation. However, the maximum drain current and the maximum transconductance of E-HEMT increase and the maximum transconductance of E-HEMT recovers to the D-HEMTs value.

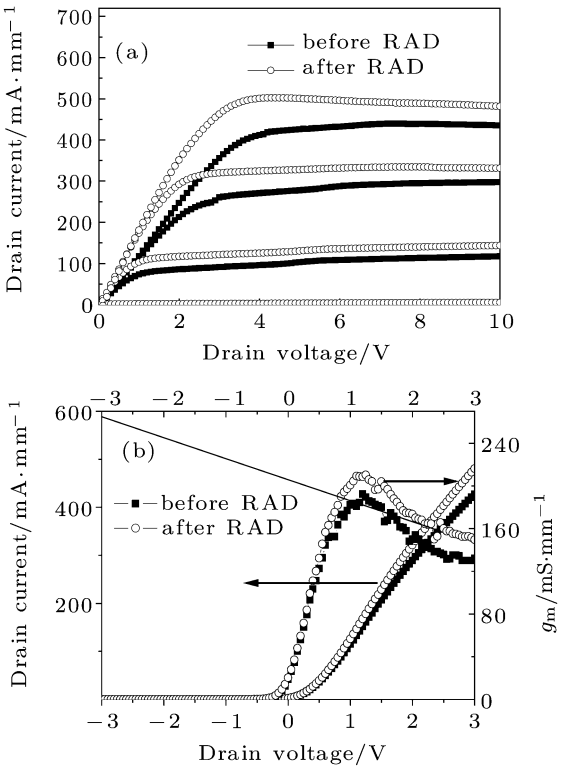


Fig. 2. (a) DC I–V output characteristics and (b) transfer characteristics of AlGaN/GaN E-HEMT before and after ^{60}Co gamma radiation.

The capacitance–voltage characteristics are used to calculate the 2DEG densities of AlGaN/GaN E-mode HEMTs (Fig. 3). The electron mobility can be deduced from the following expression:

$$R_{\rm sh} = \frac{1}{qN_{\rm s}\mu},$$

where $R_{\rm sh}$ is the sheet resistance. $R_{\rm sh}$ values of AlGaN/GaN E-HEMT before and after radiation obtained from the output characteristics and transfer line model (Fig. 2) are 958 Ω/□ and 608 Ω/□, respectively. The 2DEG density of E-HEMT keeps 0.95×10^{13} cm^{-2} during radiation. The electron mobilities of E-HEMT are 686 cm^2/(V·s) and 1081 cm^2/(V·s) before and after radiation, respectively. The device characteristic parameters of D-HEMT have no degradation after radiation. The 2DEG density is 1.1×10^{13} cm^{-2} and the mobilities are 1080 cm^2/(V·s) before radiation and 1204 cm^2/(V·s) after radiation. Electron mobility of fluorine plasma

treatment E-HEMT is degraded by fluorine etch damage. Nevertheless, it is recovered by radiation. The increase of electron mobility after radiation results in the recovery of maximum transconductance. The mobility of D-HEMT is also slightly improved after radiation, which may be due to the recovery of over CF_4 etch damage by ^{60}Co gamma radiation.

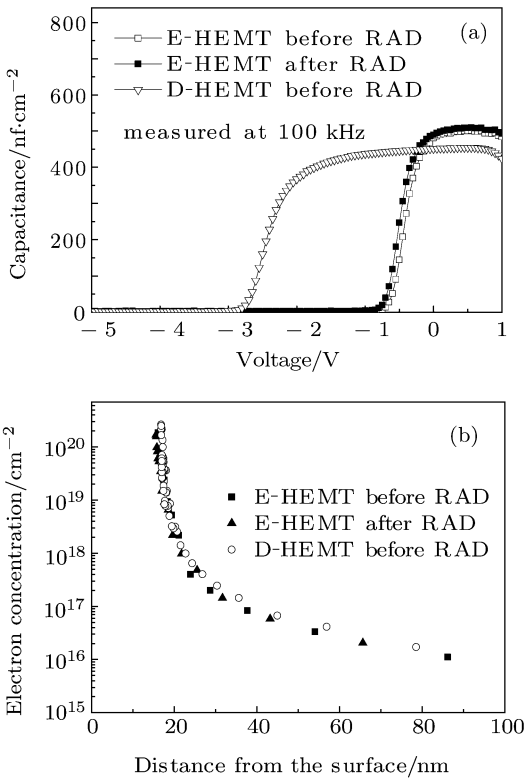


Fig. 3. (a) C–V characteristics of AlGaN/GaN Schottky gate diode before and after radiation and (b) electron distribution profile deduced from the C–V characteristics.

The conductance measurements in a frequency range from 10 kHz to 1 MHz are used to characterize the trapping effects in the D-HEMTs and E-HEMTs prepared. The equivalent parallel capacitance $C_{\rm p}$ and conductance $G_{\rm p}$ each as a function of frequency, under the assumption of a continuum of trap level, can be expressed as[15]

$$C_{\rm p} = C_{\rm b} + \frac{qD_{\rm T}}{\omega\tau_{\rm T}\tan(\omega\tau_{\rm T})},$$

and

$$\frac{G_{\rm p}}{\omega} = \frac{qD_{\rm T}}{2\omega\tau_{\rm T}}\ln[1+(\omega\tau_{\rm T})^2],$$

where $D_{\rm T}$ is the trap density, $\tau_{\rm T}$ is the trap state time constant, $C_{\rm b}$ is the barrier capacitance and ω is the radial frequency. The quantities $D_{\rm T}$ and $\tau_{\rm T}$ can be extracted by fitting the experimental data of $C_{\rm p}(\omega)$ or $G_{\rm p}(\omega)$. The conductance data are used to calculate the trap density and trap state time constant, as in this case the barrier capacitance $C_{\rm b}$ is not required to be known. Typical curves for $G_{\rm p}/\omega$ versus ω for the D-HEMT and E-HEMT, measured at selected biases near threshold voltage, are shown in Figs.4 and 5.

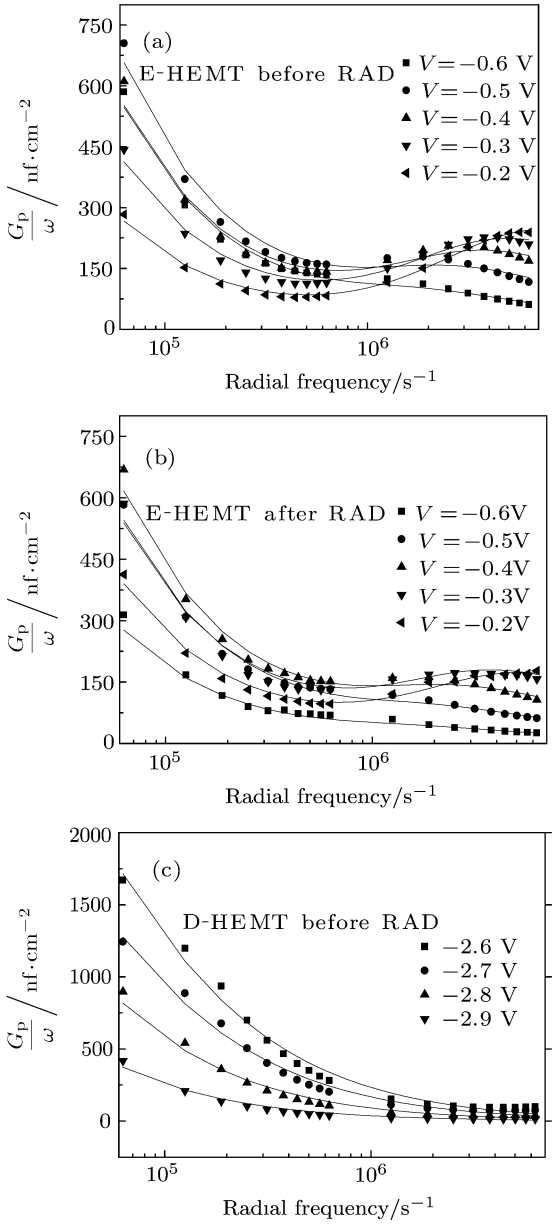


Fig. 4. Conductances each as a function of frequency for (a) E-HEMT before RAD, (b) E-HEMT after RAD and (c) D-HEMT before RAD at the gate voltages near depletion (solid lines are fitting curves).

The data for D-HEMT show one peak, which indicates that just 'slow' traps exist in the D-HEMTs. The data for E-HEMTs before and after radiation both show two peaks. This indicates that two different trap states, 'fast' and 'slow' with different densities and time constants, should be present. So the

conductance $G_{\rm p}$ can be expressed as

$$\frac{G_{\rm p}}{\omega} = \frac{qD_{\rm T(f)}}{2\omega\tau_{\rm T(f)}}\ln[1+(\omega\tau_{\rm T(f)})^2] + \frac{qD_{\rm T(s)}}{2\omega\tau_{\rm T(s)}}\ln[1+(\omega\tau_{\rm T(s)})^2].$$

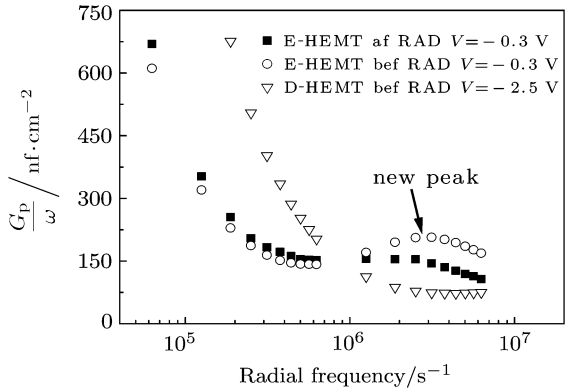


Fig. 5. Comparison of $G_{\rm p}/\omega$ versus ω curve between D-HEMT before RAD, E-HEMT before and after RAD.

The measured data are consistent with the fitted curves under the assumption of two different trap states in E-HEMT and one trap state in D-HEMT. From the fitting, the resulting parameters of the E-HEMT before radiation are $D_{\rm T(s)} = (2-6)\times 10^{12}$ cm^{-2}·eV^{-1} and $\tau_{\rm T(s)} = (0.5-6)$ ms for the slow trap state and $D_{\rm T(f)} = (1-3)\times 10^{12}$ cm^{-2}·eV^{-1} and $\tau_{\rm T(f)} = (0.2-2)$ μs for the fast trap state. From the fitting, the resulting parameters of the E-HEMT after radiation are $D_{\rm T(s)} = (2-6)\times 10^{12}$ cm^{-2}·eV^{-1} and $\tau_{\rm T(s)} = (0.5-6)$ ms for the slow trap state and $D_{\rm T(f)} = (0.2-0.8)\times 10^{12}$ cm^{-2}·eV^{-1} and $\tau_{\rm T(f)} = (0.2-2)$ μs for the fast trap state. On the other hand, fitting of $G_{\rm p}/\omega$ data for the D-HEMT yields the density of slow trap $D_{\rm T(f)} = (1-5)\times 10^{13}$ cm^{-2}·eV^{-1} with the same time constants as those for the E-HEMT.

The density of slow traps in the E-HEMT is lower than that in the D-HEMT, which shows that fluorine plasma treatment decreases the slow trap density. The slow trap time constant of several ms is consistent with that of the surface trap obtained in Ref. [16]. It was also reported that fluorine plasma treatment reduces the reverse gate leakage current.[17] The trap assistant tunneling is a dominant source of reverse gate leakage current. The decrease of the surface trap density by fluorine plasma treatment should induce the suppression of the reverse gate leakage current. So we can see that fluorine plasma treatment modifies the surface by reducing the slow traps located in the surface of AlGaN and suppresses the reverse gate leakage current.

It is also found that fluorine plasma treatment introduces a new fast trap in E-HEMT, however, this new trap was decreased by Co60 radiation. The new fast trap is a critical factor that decreases the electron mobility and degrades the maximum transconductance. With F plasma treatment, the trap is introduced by etch damage and degrades the electron mobility. The maximum transconductance of the device decreases. After ^{60}Co gamma radiation, the trap decreases and the electron mobility is improved. The maximum transconductance of E-HEMT recovers. Gamma radiation recovers the etch damage of F plasma treatment.

4. Conclusion

Conventional D-HEMT and fluorin plasma treatment E-HEMT are each fabricated on one wafer and are both exposed to ^{60}Co gamma radiation. No degradation is found in D-HEMT, nevertheless, the maximum drain current and the maximum transconductance of E-HEMT increase after radiation. Capacitance and conductance measurements are used to study the mechanism from the trap effect aspect. The results show that ^{60}Co gamma radiation decreases the new trap in E-HEMT generated by fluorine plasma treatment and recovers the maximum transconductance of E-HEMT. Both of the E/D HEMTs exhibit high stability under gamma radiation, demonstrating promising potential for GaN-based high-radiation resistant digital ICs.

References

[1] Cai Y, Cheng Z, Yang Z, Tang W C W, Lau K M and Chen K J 2007 *IEEE Electron Device Lett.* **28** 328

[2] Cai Y, Zhou Y, Lau K M and Chen K J 2006 *IEEE Trans. Electron Devices* **53** 2207

[3] Feng Q, Gu W P, Hao Y, Ma X H, Wang C and Zhang J C 2009 *Acta Phys. Sin.* **58** 511 (in Chinese)

[4] Huang S, Lin F, Liu F, Ma N, Shen B, Wang P, Wang T, Xu F J and Yao J Q 2009 *Acta Phys. Sin.* **58** 1614 (in Chinese)

[5] Duan H T, F Q, Gu W P, Hao Y, Ma X H, Ni J Y and Zhang J C 2009 *Acta Phys. Sin.* **58** 1601 (in Chinese)

[6] Cai Y, Zhou Y, Chen K J and Lau K M 2005 *IEEE Electron Device Lett.* **26** 435

[7] Cai Y, Zhou Y, Lau K M and Chen K J 2006 *IEEE Trans. Electron Devices* **53** 2207

[8] Cai Y, Cheng Z Q, Tang W C W, Lau K M and Chen K J 2006 *IEEE Trans. Electron Devices* **53** 2223

[9] Palacios T, Suh C S, Chakraborty A, Keller S, DenBaars S P and Mishra U K 2006 *IEEE Electron Device Lett.* **27** 428

[10] Yi C, Wang R and Huang W, Tang W C W, Lau K M and Chen K J 2007 *IEDM* 389

[11] Wang R N, Cai Y and Chen K J 2009 *Solid-State Electronics* **53** 1

[12] Feng Q, Gu W P, Hao Y, Ma X H, Wang C and Zhang J C 2009 *Acta Phys. Sin.* **58** 1161 (in Chinese)

[13] Membreno G A U, Dell J M, Parish G, Nener B D, Faraone L, Keller S and Mishra U K 2007 *J. Appl. Phys.* **101** 054511

[14] Wang C, Quan S, Zhang J F, Hao Y, Feng Q and Chen J F 2009 *Acta Phys. Sin.* **58** 1966 (in Chinese)

[15] Stoklas R, Gregusova D, Novak J, Vescan A and Kordos P 2008 *Appl. Phys. Lett.* **93** 124103

[16] Shen L, Palacios T, Poblenz C, Corrion A, Chakraborty A, Fichtenbaum N, Keller S, Denbaars S P, Speck J S and Mishra U K 2006 *IEEE Electron Device Lett.* **27** 214

[17] Chu R M, Shen L K, Fichtenbaum N, Brown D, Keller S and Mishra K U 2008 *IEEE Electron Device Lett.* **29** 207